



# Paperbricks produced from wastes: modeling and optimization of compressive strength by response surface approach

Abayomi Adewale Akinwande<sup>1</sup> · Davies Oludayo Folorunso<sup>1</sup> · Oluwatosin Abiodun Balogun<sup>1</sup> · Humphrey Danso<sup>2</sup> · Valentin Romanovski<sup>3,4</sup>

Received: 16 November 2021 / Accepted: 24 August 2022 / Published online: 1 September 2022  
© The Author(s), under exclusive licence to Springer-Verlag GmbH Germany, part of Springer Nature 2022

## Abstract

The high cost of building materials occasioned by the increased cost of constituent materials has contributed immensely to the problem of housing deficit faced in Africa and major developing countries of the world. Waste paper can be recycled into bricks but there are limited studies to that effect. Waste glass is used as partial cement replacement to reduce the cost of cement and is also used as a pozzolan. This study focused on the development of paperbricks from the wastes of paper and glass. Response surface method (RSM) was involved in the design of the experiment involving 4 factors: glass powder replacement of cement (A), curing duration (B), compaction pressure (C), and water/cement ratio (D). Box-Behnken method was engaged for the 4-factor, 3-level design. The result of ANOVA showed that experimental inputs had a significant effect on compressive strength response. Factors A, B, and C had a synergetic effect on the response while factor D had an antagonistic effect on the response. Combined interaction between the factors that the response depended on the interactive patterns of the factors. A statistical fit model was developed to predict the compressive strength of the composite. RSM optimization revealed a combination of 36.68%, 57.82 days, 8.50 MPa, and 0.364 for factors A, B, C, and D, respectively, predicting a strength value of 7.358 MPa. Validation experiment carried out using the optimal conditions yielded 7.54 MPa; a deviation of +0.0247. Since the deviation is less than  $\pm 0.05$ , the model was statistically validated and fit.

**Keywords** Cement · Compressive strength · Modeling · Optimization · Paperbricks · Response surface method

## Introduction

Paperbrick is an old form of brick that has gained little attention as regards its use in masonry. It was first developed in 1928 (Babu et al. 2019) but received little attention

except in recent times when it is being considered for structural application. Paperbrick is a brick of sand and cement having fibrous paper as a matrix (Akinwande et al. 2021a). This is somewhat different from papercrete in which fibrous paper is added as an additive to the concrete mix. According to Jeyakumar and Raju (2019), paperbricks are structural materials engaged in the construction of buildings. Building bricks are an essential constituent of construction, however, conventional bricks are undergoing price hikes as a result of the high demand and high cost of the constituent material. For instance, sandcrete, a blend of sand and cement is becoming more expensive owing to the scarcity of sand which is a major constituent. Cement also is experiencing a price rise on account of the high cost of production. These have led to the high cost of construction, resulting in a high housing deficit. As such, cheaper alternatives are being sourced to tackle this challenge.

The housing deficit in Africa and most developing countries of the world keep rising with time (Ofori 2020). In Nigeria, for instance, there existed a gradual rise in

---

Responsible Editor: Philippe Garrigues

✉ Abayomi Adewale Akinwande  
abypublications@gmail.com

<sup>1</sup> Department of Metallurgical and Materials Engineering, Federal University of Technology, Akure, Nigeria

<sup>2</sup> Department of Construction and Wood Technology, Akenten Appiah-Menka University of Skills Training and Entrepreneurial Development, Kumasi, Ghana

<sup>3</sup> Center of Functional Nano-Ceramics, National University of Science and Technology «MISIS», Lenin av., 4, 119049 Moscow, Russia

<sup>4</sup> Department of Materials Science and Engineering, University of Virginia, Charlottesville, VA 22904, USA

a housing deficit of 7 million in 1991 to 14 million in 2010 according to a World Bank report (World Bank 2018). The report further claimed that Nigeria required 700,000 annual housing units for 20 years to be able to curb the challenge of the housing deficit. Presently in 2021, a value of 22 million deficits is recorded (Pona et al. 2021). Unfortunately, the problem keeps persisting on account of the lack of decisive attempts of government in tackling the challenge. Over 50% of Nigerians are reported to stay in slums and shanties portending great danger in respect to outbreaks of diseases (Obaitor et al. 2021; Joshua and Glanda 2016). There is a need for a decisive solution pertaining to the present challenge.

According to Solaja et al. (2020), to solve the problem at hand, a cheaper alternative is the way to go which involves waste recycling (Hurynovich et al. 2021). Wastes are often used in the production of materials for different purposes: modified materials for water treatment (Romanovski et al. 2021a), wastewater treatment (Bakhsh et al. 2022), recovery of metals (Matsukevich et al. 2022), pigments (Zalyhina et al. 2021a, 2021b), as well as building materials, such as gypsum (Romanovski et al. 2022; Kamarou et al. 2021a), anhydrite (Kamarou et al. 2021b; Romanovski et al. 2021b), bricks (Zalyhina et al. 2022), etc. This assertion is supported by Mohammed et al. (2020). In recent years, waste paper (WP) recycling is gaining more attention, especially for structural applications. Diverse researches have been undergone in this area to convert WP to bricks. Almost 4 billion trees are cut down yearly in the making of paper worldwide (Arya and Kansal 2015). These papers are majorly in form of office papers, newspapers and cardboards which have short-term use. Unfortunately, the wastes are dumped in landfills as a form of disposal. Zaki (2019) claimed over 500 million tons of WP are produced worldwide. Rather than their disposal, they can be reduced, reused, and recycled into other useful forms, one of which is paper-cement composite meant for construction.

A major concern of paperbricks is the ability to carry the load (compressive strength) and the challenge of water susceptibility due to hydrophilicity and hygroscopicity. Raoelivololona et al. (2020) supported the recycling of paper into bricks for affordable low-cost construction. Investigation carried out by Sangrutsamee et al. (2012) upheld Raoelivololona et al. (2020) assertion. In the study, WP was repulped into a paper-cement composite for building application on account of the low thermal conductivity of the material. WP has been confirmed to have some advantages over concrete or sandcrete bricks in terms of low cost, eco-friendliness and lightweight (Liladia et al. 2020). Rani et al. (2018) compared conventional sandcrete bricks with developed paperbricks. In the study, it was established that paper-cement composite bricks are lighter and cheaper than conventional bricks. The good damping property of

paper pulp based on the inherent cellulose fiber gives it consideration for construction works in comparison with sand-brick or clay-bricks.

Different studies have developed the bricks made from WP for masonry application. Arya and Kansal (2015) developed paper-based bricks by the mixture of cement and the pulp itself. Curing was carried out for 14, 21, and 28 days. It was noted that increasing curing periods engendered strength enhancement and reduction in water assimilation. A similar experience was reported in the investigation carried out by Delcasse et al. (2017) in that higher curing age ensued better performance in the bricks. Okeyinka et al. (2015) designed lightweight block from newspaper by infusion of cement additive to a paper pulp at 0, 4, 8, 12, 16, and 20 wt.%. The sand was also varied from 0 to 20 wt.% at 4 wt.% interval. As observed, increasing binder enhanced strength, same with sand proportion. Compressive strength was concluded to be affected by the interaction between cement and sand. Mandilli et al. (2020) produced bricks from WP and a cement blend. Cement was added to the pulp at 10, 20, 30, 40, 50, and 60 wt.%. As observed in the study, density, compressive, and flexural strength increased progressively with percentage rise in cement. Ultrasonic pulse velocity was also noted to show a linear increase with cement proportion. Ahmad et al. (2021) also blended cement and sand with paper pulp in the development of paperbricks. The result portrayed that higher cement content increased strength performance while water absorption was reduced with cement content. From the literature, it is observed that cement is an essential binder and strengthener in the design of the bricks. However, high cement content of between 40 and 60% was employed for strength optimization. The use of such an amount of cement seems too high knowing fully well that the price of cement is on the rise. The high cost of cement is one of the challenges faced in the building industry. Therefore, it is better to access ways of lowering the content and at the same time, maintain the strength. One way forward in this regard is the introduction of pozzolan such as glass powder. This concept has drawn attention in many studies as a way of lowering the cost of cement used in concrete and at the same time initiate pozzolanic reaction (Nyantakyi et al. 2020; Sadiqul Islam et al. 2017; Carbo et al. 2021).

Waste glass is nonbiodegradable and is dumped on landfills contributing to environmental degradation (Ferronato and Torretta 2019; Olofinnade et al. 2018). Therefore, recycling by way of its inclusion in cement composite as a pozzolan is a justified initiative. More so, glass powder being a silica base material undergoes pozzolanic reaction as carried out in previous studies (Zheng 2016; Tamanna et al. 2016; Najad et al. 2019). Pozzolan is a siliceous and aluminous material that in powdery form reacts with hydrated lime in the presence of water to form calcium silicate hydrate (C-S-H). Hydrated lime constitutes up to 25%

of the hydration product of cement and does not contribute to the strength of cement composite (Wang 2019). Via pozzolanic reaction, the lime transforms to C-S-H, a very useful hydrate for the long-term strength of the composite. That implies that a lower proportion of cement, when combined with a pozzolan, can yield interesting results in maintaining or enhancing the strength of cement composite. This concept births the use of glass powder (GP) as a partial replacement of cement in this study.

Curing duration is another factor for strength optimization. Most of the reviewed studies cured samples for an utmost of 28 days; however, curing beyond such duration may be necessary. This is because the paper is majorly a cellulose (sugar compound) base material and these compounds delay hydration in cement composite (Kassa 2019; Shahidkha and Singh 2018). In that case, it implies that optimum strength beyond 28 days is possible and worth investigating. Curing duration range of 30 to 60 days was adopted on account of research studies of (Akinwande et al. 2021a, b). Most works involving paperbricks development hardly consider compaction pressure during the production process and it is necessary because of the effect on the performance of the bricks. In the present investigation, compaction pressure was varied between 4 and 10 MPa according to range value (between average and high moulding pressure) stipulated in (Danso 2015). Water/cement ratio is another experimental variable that also demands attention to determining the optimum ratio for paperbrick development. In concrete, a lower water/cement ratio reduces the workability of the mix leading to segregation and uneven dispersion of aggregate (Panda et al. 2020). On the other hand, a high water/cement ratio spawns increase in porosity amounting to lower compressive strength. Consequently, upon that, a moderate water/cement ratio is employed, hence the range of 0.4 to 0.7 was specified. As in the case of paperbricks, there is no stipulated value for the water/cement ratio, requiring more study in that aspect. This is necessary owing to the hydrophilic tendency of paper, which means that the range of value for concrete may need to be lesser in the case of Paperbricks. Therefore, there is a need to access the optimum water/cement ratio to design paperbricks. The range value of 0.36 to 0.42 was chosen based on a previous study (Akinwande et al. 2021a, b). Glass powder (GP) replacement of cement at 40 wt.% cement by weight of paper pulp.

A very important property that determines the service performance of bricks or any cement composite is compressive strength and the same is the focus of this investigation. There are four experimental factors considered in this study about compressive strength. They are glass powder replacement of cement, curing duration, compaction pressure and water/cement ratio. For good experimental management, the response surface method (RSM) of the design of the experiment was engaged in the design of the experiment and

optimization of the result. This study, therefore, focused on the experimental design of paperbricks at different combinations of input variables onto modelling and optimizing the compressive strength.

## Materials and methods

### Material preparation and specimen development

Waste papers used in this study were obtained from a book store where old papers were packed. The papers were shredded, soaked in water for 7 days, drained and packed before grinding using a paper grinding machine. The slurry was transferred into a sack and the sack was subjected to a pressure of 10 MPa to drain water. The pulp was spread in the open air for 14 days to dry. Afterward, the dried pulp was collected for sample preparation. Figure 1 at right side shows an SEM image of the pulp featuring presence of meso and microcapillary pores. These observed features are held responsible for their porosity and hydrophilicity.

River sand was collected and treated by subjecting it to water treatment. Water was added, stirred and the mixture left for 24 h. The supernate was poured off and the process was repeated twice. Leftover sand was oven-dried at 110 °C for 24 h and collected for milling. With the use of a ball mill, collected sand was milled, after which it was sieved to – 150 µm. Fine sand milled to – 150 µm was collected and employed in composite development. Waste glass bottles were collected from a merchant store, washed and grinded before been pulverized. This was followed by sieving to – 75 µm before being oven dried at 110° for 5 h and employed for preparation of samples. Binder employed in this study is ordinary Portland cement (grade 43), obtained from an open shop. The cement was evaluated for inherent properties to ascertain its conformity with IS 8112 (IS 8112, 2013). Levels of factors considered in the design of the experiment are stipulated in Table 1.

### Sample preparation

Reference brick samples were produced as the blend of 40 wt.% cement, 20 wt.% sand by weight of paper pulp, and cured for 30, 45, and 60 days (Fig. 1). Water cement ratio and compaction pressure were maintained at zero level, 0.39 and 5 MPa, respectively. Other samples for analysis were prepared according to the runs stipulated in Table 2. GP replacement was introduced as partial replacement of the 40 wt.% cement (by weight of the pulp) in line with experimental runs in Table 2. Sand proportion was maintained at 20 wt.% by weight of the pulp for all samples produced. Mixing was done in a mechanical mixer of cylindrical shape. The mix was transferred into 150×150 mm cube moulds and compacted at

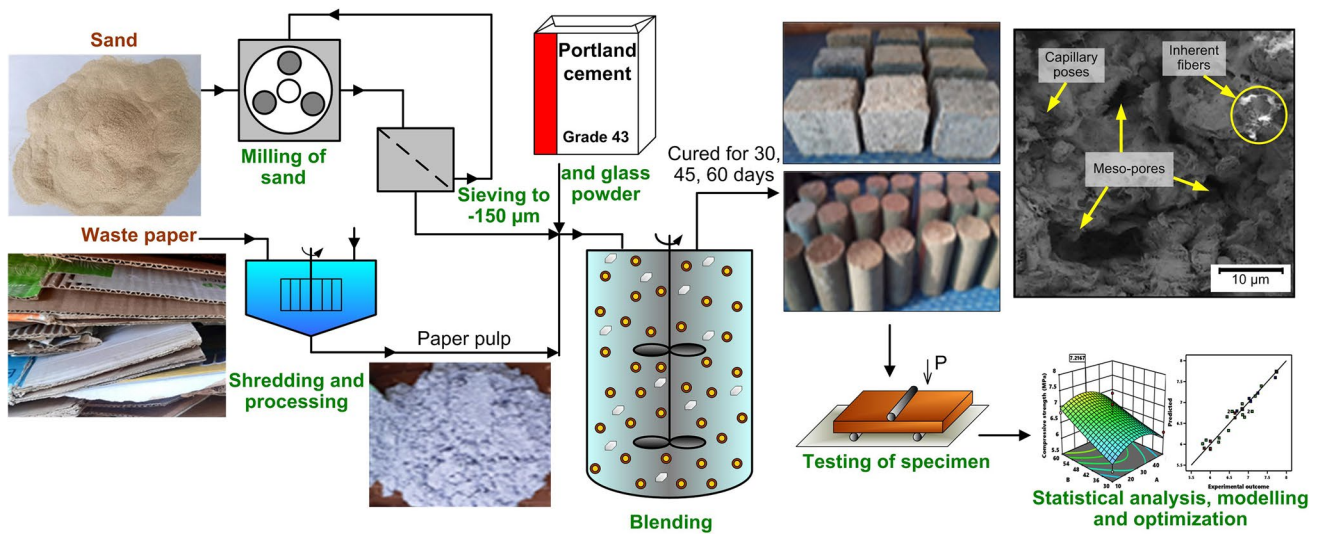


Fig. 1 Schematics of the paperbricks composite production process

Table 1 Levels of factors in the design of experiment

Factors	Low level (− 1)	Medium level (0)	High level (+ 1)
Percentage replacement (A)	10%	30%	50%
Curing duration (B)	30 days	45 days	60 days
Compaction pressure (C)	4 MPa	7 MPa	10 MPa
Water/cement ratio (D)	0.36	0.39	0.42

pressures stated in Table 2 for 5 min. Specimen were carefully removed from the moulds and cured for different days specified in the experimental runs (Table 2) in line with ASTM C 192/C 192 M (ASTM C 192/C 192 M 2019). Schematic of the procedure is revealed in Fig. 1 and represent the produced brick samples. Curing was done by covering bricks with polyethylene bags kept in a plastic container for the number of days stipulated in Table 2.

**Experimental design and procedure**

Response surface method (RSM) is a statistical and mathematical tool which accesses the relationship between experimental inputs and how the interaction affects behavior of the response (Zhang and Zhai 2020; Zhang and Yue 2018; Ebadi et al. 2019). It is a useful tool in optimization procedures (Shabani et al. 2018). Box-Behnken design of the RSM only needs 3 point or level in the design space to access effect of a given factor on the response. The points are termed low, medium, and high. In response surface, a second-order polynomial expression is often employed as model expression of the response as a function of the factors. Equation 1 represents a typical model expression for a four factor-three level design as employed in this study.

$$\begin{aligned}
 Y = & Z + mA + mB + mC + mD + mAB \\
 & + mAC + mAD + mBC + mBD + mCD \\
 & + mAA + mBB + mCC + mDD
 \end{aligned}
 \tag{1}$$

where Y is the response, m is the coefficients, A, B, C, and D are factors influencing the response while AA, BB, CC, and DD are square interactions and AB, AC, AD, BC, BD, CD are cross interactions. The statistical fitness of the model can be derived from the ANOVA and diagnostic report.

In the present study, experimental factors are percentage replacement (A, %), curing duration (B, days), compaction pressure (C, MPa), and water/cement ratio (D). The 4-factor, 3-level experimental design and run analysis was carried out using Design-Expert 13. The response was compressive strength which was probed in line with IS 516 (IS 516 2004) and obtained through Eq. (2). The 150 × 150 mm cube samples were subjected to compressive test using a universal testing machine (model: Instron 3382 A) at a loading rate of 30 kN/min.

$$\text{Compressive strength} = \frac{\text{Maximum load (P)}}{\text{Cross – sectional area (A)}}
 \tag{2}$$



**Table 2** Coded levels and factors

Runs	Coded levels				Factors				Response
	A	B	C	D	A	B	C	D	Compressive strength (MPa)
1	-1	0	-1	0	10	45	4	0.39	3.91
2	-1	0	0	1	10	45	7	0.42	3
3	0	0	0	0	30	45	7	0.39	5.88
4	0	0	0	0	30	45	7	0.39	5.91
5	1	0	1	0	50	45	10	0.39	6.03
6	-1	-1	0	0	10	30	7	0.39	3.91
7	0	1	-1	0	30	60	4	0.39	5.78
8	0	0	-1	-1	30	45	4	0.36	6.07
9	0	0	1	1	30	45	10	0.42	5.69
10	1	1	0	0	50	60	7	0.39	5.9
11	1	0	-1	0	50	45	4	0.39	4.82
12	0	0	-1	1	30	45	4	0.42	4.49
13	0	-1	-1	0	30	30	4	0.39	4.8
14	1	0	0	-1	50	45	7	0.36	6.2
15	0	0	1	-1	30	45	10	0.36	7.27
16	1	0	0	1	50	45	7	0.42	4.6
17	0	1	1	0	30	60	10	0.39	7
18	0	0	0	0	30	45	7	0.39	5.9
19	1	-1	0	0	50	30	7	0.39	4.91
20	0	1	0	1	30	60	7	0.42	5.6
21	0	-1	0	-1	30	30	7	0.36	6.22
22	0	-1	1	0	30	30	10	0.39	6.01
23	-1	0	0	-1	10	45	7	0.36	4.5
24	-1	1	0	0	10	60	7	0.39	4.89
25	0	-1	0	1	30	30	7	0.42	4.6
26	0	1	0	-1	30	60	7	0.36	7.2
27	-1	0	1	0	10	45	10	0.39	5.04

## Results and discussion

### Preliminary result on input materials

Figure 2a represents the microstructural image carried out using a scanning electron microscope (JSM-7610) featuring ranging sizes. The spot EDX result for fine sand (FS) is indicated in Fig. 2b. The result showcased the presence of calcium, aluminium, carbon, oxygen, magnesium, and others which corresponds with results observed in the literature (Devi et al. 2013; Wang et al. 2019). Silicon shares the highest amount while oxygen followed. This suggests the occurrence of silica ( $\text{SiO}_2$ ) and alumina ( $\text{Al}_2\text{O}_3$ ), constituents of river sand. The phases are identified in the XRD diffraction plots (Fig. 2c) showing peaks of mica, alumina, and quartz ( $\text{SiO}_2$ ) as confirmed in literature (Muttashar et al. 2018).

The chemical composition of the sand obtained by XRF in Table 3 further corroborates existing results. Major chemical contents present are  $\text{SiO}_2$  (71.5%),  $\text{Al}_2\text{O}_3$

(15.6%), and other elements confirming silica-based sand. Figure 2d shows the particle size distribution of the fine sand (FS) which was sieved to  $-150\ \mu\text{m}$ . From the graph, 42.8% of the sand passed through the  $-150\ \mu\text{m}$  sieve indicating well-graded sand. Fineness modulus was determined to be 1.67 and with regards to IS 383 (IS 383 1970), the sand is termed grade III sand; implying moderate fineness. Particle size analysis was further carried out to determine the average size of FS employed, the value of which was  $122.11\ \mu\text{m}$  (Fig. 2e). Figure 2f presents the SEM image of the glass powder employed in this study. The sizes slightly varied, mostly spherical in shape. From the EDX result (Fig. 2g), peaks of Si, Al, O, and Ca are observed with proportions of 45.7, 12.87, 20.4, and 8.20 wt.%, respectively. Compounds present are  $\text{SiO}_2$ ,  $\text{Al}_2\text{O}_3$ , CaO, and FeO, confirming the result of Table 3. In the table,  $\text{SiO}_2$ ,  $\text{Al}_2\text{O}_3$ , and CaO share 67.6, 12.3, and 8.6%, respectively. According to ASTM C 618 (ASTM C 618 2019), addition of  $\text{SiO}_2$ ,  $\text{Al}_2\text{O}_3$ , and FeO must be  $\geq 70\%$  for a pozzolan. The glass powder employed in

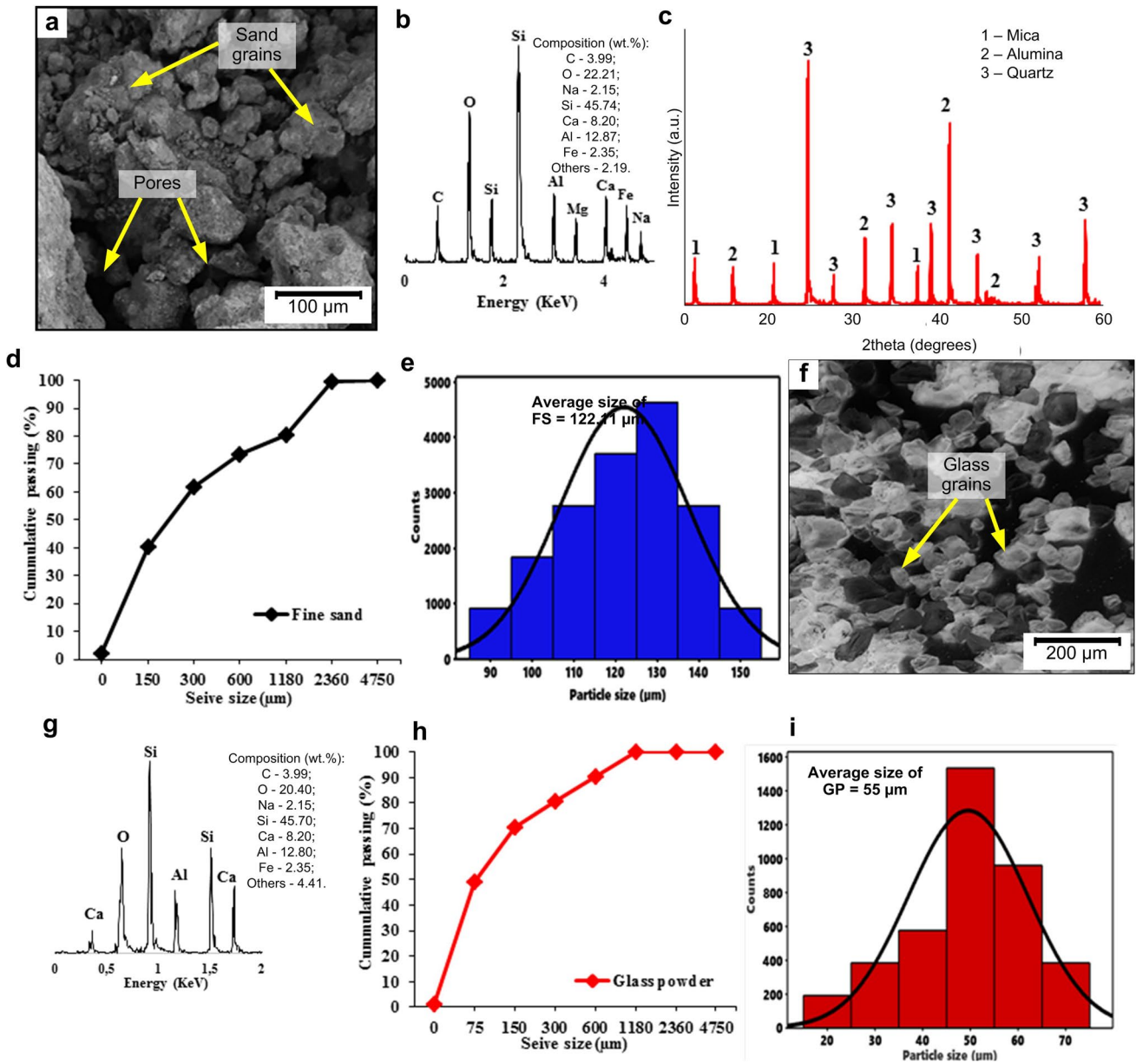


**Fig. 2** Properties of sand and glass powder employed in the study as presented by **a, b** microstructural SEM image of fine sand and EDX for elemental composition of fine sand, **c** phase identification by XRD for fine sand, **d, e** particle size distribution and particle size analysis

for fine sand, **f, g** microstructural SEM image of glass powder and EDX for glass powder, and **h, i** particle size distribution and particle size analysis glass powder

**Table 3** Chemical composition of milled sand

Chemical compounds												
Composition	SiO <sub>2</sub>	Al <sub>2</sub> O <sub>3</sub>	CaO	Na <sub>2</sub> O	MgO	Fe <sub>2</sub> O <sub>3</sub>	TiO <sub>2</sub>	K <sub>2</sub> O	MnO	SO <sub>3</sub>	Others	LOI
Fine Sand (%)	71.5	15.6	0.41	1.34	0.21	2.11	0.89	0.15	1.94	-	4.64	1.21
Glass powder (%)	67.6	12.3	8.6	4.3	0.34	1.55	-	0.06	1.2	-	2.95	1.10
Cement (%)	20.54	4.96	63.15	-	1.96	3.00	-	-	1.20	2.42	1.05	1.72

this study is deduced to satisfy the requirement. Figure 2h is the particle size distribution chart (Fig. 2h) for glass powder (GP). 48.6% of the GP passed through the  $-75\ \mu\text{m}$  sieve even as obtained from the particle size analysis (Fig. 2i) average size of  $55\ \mu\text{m}$ . The chemical composition of the cement is illustrated in Table 3 with CaO having the highest proportion.  $\text{SiO}_2$  was also present in high proportion.

According to Table 4, sand, glass powder, and cement have a specific gravity of 2.62, 2.84, and 3.17 indicative of the fact that cement is the heaviest, next is glass powder while sand is lighter than the two. Moisture content for sand is highlighted as 4.2%. Cement is determined to be the finest with fineness a modulus of 1.22. The glass powder is finer than sand with a fineness modulus of 1.39 even as sand has a 1.65 fineness modulus. In terms of a specific area, cement has the highest while glass powder is followed. With a high specific area, the pozzolanic reaction is promoted for strength optimization.

**Table 4** Physical properties of the fine sand, glass powder, and cement

Properties	Specific gravity	Moisture content	Fineness modulus	Specific area
Sand	2.62	4.2	1.65	1745 $\text{cm}^2/\text{g}$
Glass powder	2.84	-	1.39	2367 $\text{cm}^2/\text{g}$
Cement	3.17	-	1.22	3578 $\text{cm}^2/\text{g}$

**Table 5** Analysis of variance (ANOVA) on compressive strength

Source	Sum of squares	df	Mean square	F value	p value	Contribution (%)
Model	27.06	14	1.93	49.19	<0.0001	98.29
A-Cement replacement	4.33	1	4.33	110.26	<0.0001	15.74
B-Curing duration	2.92	1	2.92	74.34	<0.0001	10.61
C-Compaction Pressure	4.28	1	4.28	109.04	<0.0001	15.56
D-W/C ratio	7.49	1	7.49	190.62	<0.0001	27.21
AB	0.0000	1	0.0000	0.0006	0.9803	
AC	0.0016	1	0.0016	0.0407	0.8435	
AD	0.0025	1	0.0025	0.0636	0.8051	
BC	0.0000	1	0.0000	0.0006	0.9803	
BD	0.0001	1	0.0001	0.0025	0.9606	
CD	0.0000	1	0.0000	0.0000	1.0000	
A <sup>2</sup>	6.29	1	6.29	160.18	<0.0001	28.54
B <sup>2</sup>	0.0147	1	0.0147	0.3742	0.5522	
C <sup>2</sup>	0.0217	1	0.0217	0.5517	0.4719	
D <sup>2</sup>	0.0768	1	0.0768	1.95	0.1874	
Residual	0.4715	12	0.0393			
Lack of fit	0.4710	10	0.0471	201.85	0.0949	1.71
Pure error	0.0005	2	0.0002			
Cor total	27.53	26				
$R^2=0.9829$		Adj $R^2=0.9629$		Adj $R^2=0.9014$		Adeq. Pres = 26.42

## Results on developed composite

Analysis of variance was effected to evaluate contributions of the linear, quadratic, and interaction terms on compressive strength response. The result of the ANOVA of the developed paperbrick composite is highlighted in Table 5. The  $F$ -value of the model term is 49.19 indicating a 0.01% probability of the value occurring due to noise. Equally, the  $p$  value of the model ( $p < 0.0001$ ) means the model showed a good relationship with the residual. As observed, the variables are significant, since  $p < 0.05$ . In that case, input variables; percentage replacement (A), curing duration (B), compaction pressure (C), and water/cement ratio (D) had a significant contribution to the response. The parameters AB, AC, AD, BC, BD, CD, BB, CC, and DD had  $p$  value  $> 0.05$ ; therefore, their respective contributions to the response are insignificant. However, that of AA is  $< 0.05$ , indicating that the contribution is significant. Also, lack of fit showed a  $p$  value of 0.8601 ( $p > 0.05$ ) depicting lack of fit to be insignificant, the implication of which confirmed the model to be statistically adequate to represent the data. Residual correlation coefficient  $R^2$  is 0.9829 pinpointing a significant correlation exists between the response model and the residuals. The representation of the data by the model is said to exhibit 98.29% dependability with 1.71% (insignificant) diversion from the fit. Difference in value between adjusted  $R^2$  (0.9629) and predicted  $R^2$  (0.9014) is  $< 0.2$ , presenting a

good correlation. Adeq. precision estimates the amount of signal-to-noise ratio (S/N) (Silantsev et al. 2019). The value is 26.42, indicating that the signal is 26.42 times greater than the noise. This further shows the model to be competent in the navigation of design space.

The contribution of each experimental input is stated in Table 5. Percentage replacement of cement, curing duration, compaction pressure, and water/cement ratio shared 15.74, 10.61, 15.56, and 27.21%, respectively. Consequently, the descending order of contributions of the input parameters is water/cement ratio, percentage replacement of cement, compaction pressure, and curing duration. Meanwhile, interaction AA shared 28.54% contribution on compressive strength.

The predictive model via multi regression analysis of the experimental outcome is stated in Eq. 3.

$$\begin{aligned}
 CS = & -9.70698 + 0.2065A + 0.0069B + 0.0875C \\
 & - 78.4167D + 0.0000AB + 0.0003AC - 0.0417AD \\
 & + 0.0001BC + 0.0111BD + 0.0000CD - 0.0027AA \\
 & + 0.0002BB + 0.0071CC - 133.3333DD
 \end{aligned}
 \tag{3}$$

From the equation, terms with a positive coefficient had a positive influence on the response while the negative coefficient depicts a negative influence on the response. To this end, factors A (percentage replacement), B (curing duration), and C (compaction pressure) had a synergetic effect on compressive strength response. The water/cement ratio (D) showed an antagonistic effect on compressive strength response.

The adequacy of a model is determined using a normal plot as presented in Fig. 3. When the residuals fall on a straight line, then the residuals are distributed normally

**Fig. 3** Diagnostics plots on compressive strength represented by **a** normal plot **(b)** residuals vs run plot **(c)** predicted vs actual plot **(d)** perturbation plot

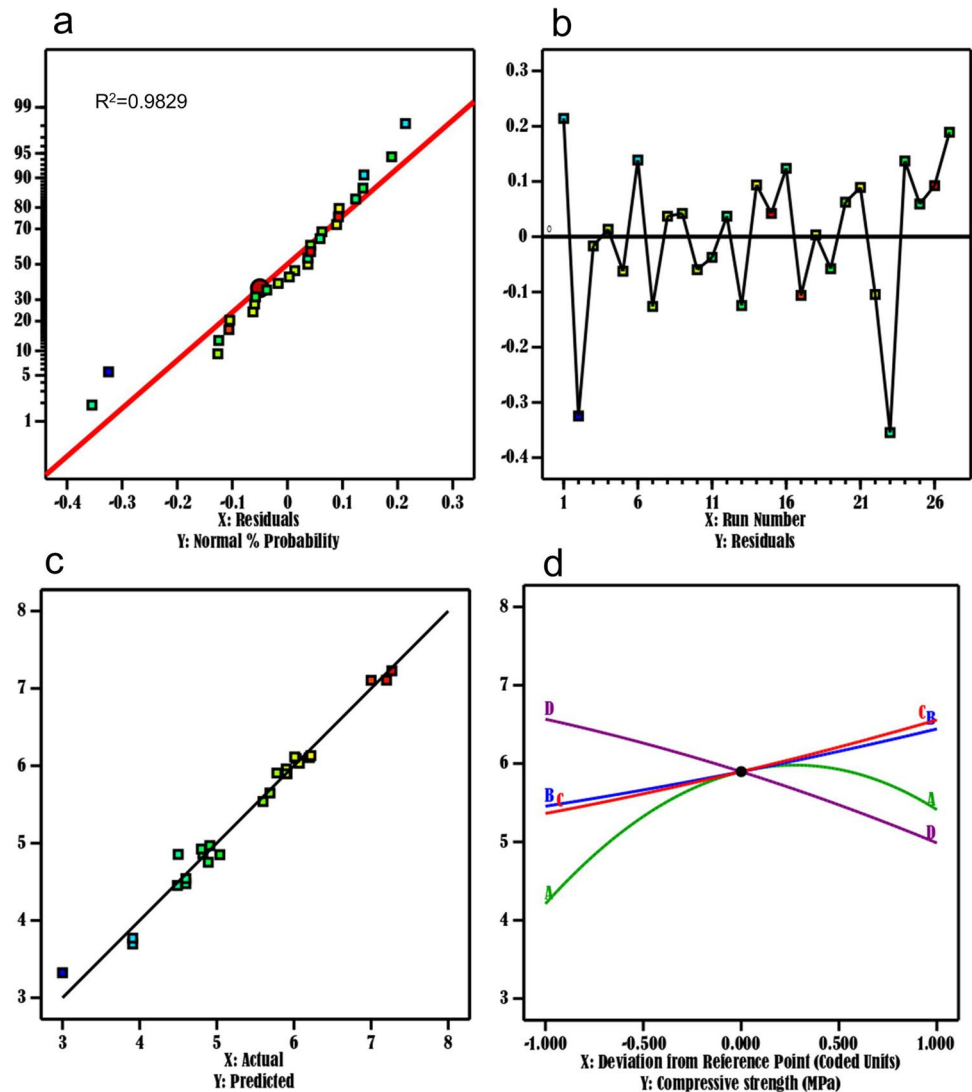
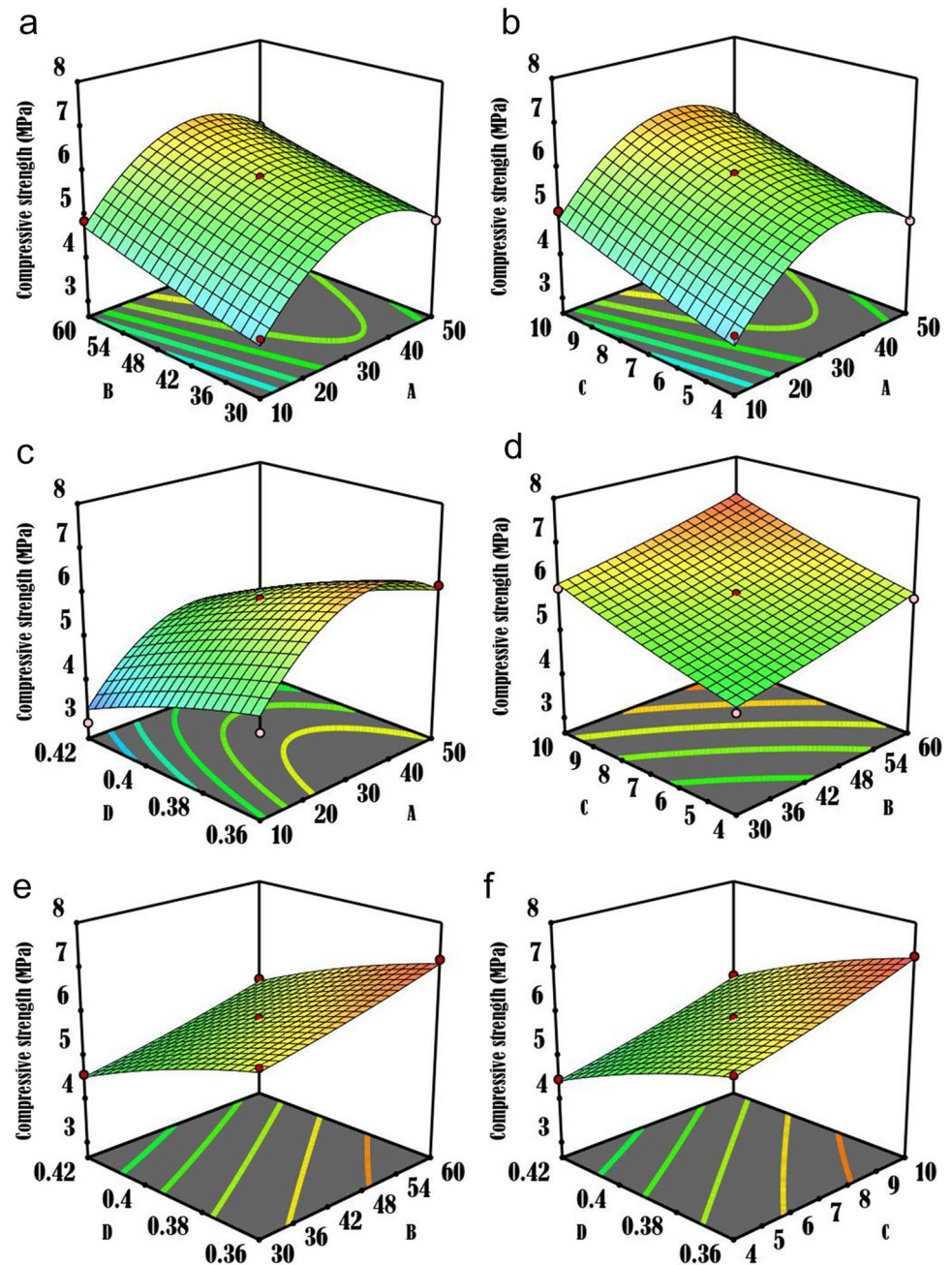




**Fig. 4** Interactions between process parameters and their effect on compressive strength of developed paperbricks as represented by response surface plot: **a** percentage replacement vs curing duration, **b** percentage replacement vs compaction pressure, **c** percentage replacement vs water/cement ratio, **d** curing duration vs compaction pressure, **e** curing duration vs water/cement ratio, **f** compaction pressure vs water/cement ratio. Here, A is percentage replacement (%), B is curing duration (days), C is compaction pressure (MPa), and D is water/cement ratio



(Khare et al. 2018). Figure 3a signifies that the residuals are normally distributed along the line. Figure 3b illustrates the residuals vs run order meant to affirm whether the residuals are independent of one another. The residuals are scattered around the zero-horizontal line. This means that the plot shows no trend or pattern for the residuals when revealed in time order thereby affirming the residuals are not correlated.

Figure 3c highlights the predicted vs actual (experimental outcome) plot. The values are cited evenly at both sides of the line (plotted at 45° to the horizontal). That being the case, the model is statistically fit to predict compressive

strength responses. A perturbation plot is meant to examine the effects of the factors at a fixed point in the design space as demonstrated in Fig. 3d. The response was plotted varying one factor at a time over its range values while maintaining constant value for other factors. The reference point set in this study is coded 0 (midpoint) as observed in the figure. As demonstrated, factor A shows a curvature from  $-1$  to  $+1$  (low to high), B and C reflect a linear progressive increase from low to high while factor D depicts a progressive decrease from  $-1$  to  $+1$ .

A surface plot is a 3-dimensional representation that shows the relationship between a response (dependent

variable) and independent factors (Husuma and Mahfud 2016; Akinwande et al. 2022a). The plot is such that the response is plotted on the Z-axis while the factors are plotted on the X- and Y-axis. The plot reflects the effect of the interaction between the X and Y variables on the response plotted on the Z-axis. Figure 4 represents the response surface plots of the effect of combined interactions between the parameters as they affect compressive strength response.

#### **Influence of interactions between percentage replacement (A) and curing duration (B) on compressive strength of the composite**

Figure 4a showcases the response surface plot of the influence of the combined interaction between percentage replacement and curing duration on compressive strength at a constant compaction pressure of 7 MPa and water/cement ratio of 0.39. As cement is replaced by GP at a replacement proportion of 10 to 30%, there was an appreciable increase in compressive strength. Meanwhile, the strength reduced when the replacement proportion increased from 30 to 50%. On another hand, the compressive strength increased progressively from 30 to 60 days. Interaction between factors A and B is explained thus. The simultaneous increase in percentage replacement between 10 and 30% and curing duration of 30 to 60 days ensued improvement in strength; however, the combination of percentage 30 to 50% and curing duration of 30 to 60 days led to strength reduction. It is affirmed that the compressive strength of the developed composite depends on the interactive pattern between the parameters. Percentage replacement depicted a parabolic profile of inverted “U” shape. The point of inflexion was at 30% replacement and curing duration of 60 days yielding 6.45 MPa. Curing duration, on the other hand, portrayed a positive linear profile as days increased from 30 to 60 days.

#### **Influence of interactions between percentage replacement (A) and compaction pressure (C) on compressive strength of the composite**

Figure 4b illustrates the interaction percentage replacement (A) vs compaction pressure (C) at a constant curing duration of 45 days and a water/cement ratio of 0.39. Increasing replacement proportion of 10 to 30% resulted in strength enhancement while between 30 and 50%, there was strength reduction. An increase in compaction pressure amounted to progressive strength enhancement from 4 to 10 MPa. Therefore, interaction ranging from 10 and 30% GP replacement proportion and compaction pressure between 4 and 10 MPa prompted improvement in compressive strength. Thirty to 50% GP replacement proportion in the composite compacted applying pressure of 4 and 10 MPa yielded strength reduction. Replacement proportion delineated an inverted U-shaped parabolic interaction profile. Point of inflexion was noted when compressive strength of

6.635 MPa corresponding with 30% GP replacement proportion and curing age of 45 days. Compaction pressure depicted a positive linear interaction profile between 4 and 10 MPa. The strength is dependent on the interaction profile between percentage replacement (A) and compaction pressure (C).

#### **Influence of interactions between percentage replacement (A) and water/cement ratio (D) on compressive strength of the composite**

Figure 4c features the interactive pattern of the relationship percentage replacement vs water/cement ratio when holding curing duration and compaction pressure at 45 days and 30% respectively. As observed, 10 to 30% percentage replacement resulted in strength enhancement even as 30 to 50% replacement proportion yielded strength reduction. In that case, percentage replacement exhibits a parabolic profile of inverted U shape. As the water/cement ratio increased from 0.36 to 0.42, it was observed that strength was lowered. The water/cement ratio displayed a negative linear interaction profile. Hence, there is an inverse interaction at the combined interplay between 10 and 30% percentage replacement and 0.36 to 0.42 water/cement ratio. Meanwhile, 30 to 50% percentage GP replacement interplaying with 0.36 to 0.42 water/cement ratio depicted a downward interaction between the two parameters. Points of inflection yielded maximum strength of 6.278 MPa, corresponding with a 30% GP and 0.36 W/C ratio. The response is said to be dependent on the interaction profile of the percentage replacement (A) and water/cement ratio (D).

#### **Influence of interactions between curing duration (B) and compaction pressure (C) on compressive strength of the composite**

Effects of the interactivity between curing duration and compaction pressure when holding percentage replacement and water/cement ratio at 45 days and 30% respectively are displayed in Fig. 4d. An increase in curing duration from 30 to 60 days amounted to strength improvement. Equally, increase in compaction pressure from 4 to 10 MPa engendered improvement in strength. Consequently, the relationship between 30 and 60 days curing duration and compaction pressure of 4 to 10 MPa had a synergetic effect on the response. The two factors, curing duration and compaction pressure paraded positive linear interaction profile. It is concluded that compressive strength is dependent on the interaction pattern of factors B and C.

#### **Influence of interactions between curing duration (B) and water/cement ratio (D) on compressive strength of the composite**

The outcome of the interrelation curing duration vs water/cement ratio as it affects compressive strength at constant

GP percentage replacement of 30% and compaction pressure of 7 MPa is outlined in Fig. 4e. As noted in the figure, 30 to 60 days' duration had a positive influence on boasting strength while water/cement ratio 0.36 to 0.42 is detrimental to strength. There is an inverse linear interaction between the two factors as they affect compressive strength. The two displayed linear interaction profile; while curing days exhibited a positive linear profile, the water/cement ratio manifested a negative linear interaction profiles. Compressive strength response is verified to be dependent on the interactive pattern between the two parameters. Maximum compressive strength of 7.1 MPa for the interaction was achieved at coordinates of 60 days curing duration and 0.36 W/C ratio.

### Influence of interactions between compaction pressure (C) and water/cement ratio (D) on compressive strength of the composite

The efficacy of the interplay compaction pressure vs water/cement ratio on compressive strength at constant percentage replacement of 30% and curing duration of 45 days is denoted in Fig. 4f. An increase in compaction pressure from 4 to 10 MPa begat improvement in compressive strength. Meanwhile, progressive rise in water/cement ratio expresses progressive linear reduction in strength. In that case, there exist inverse linear interaction between the factors. The two factors C and D expressed a linear interaction profile. As factor C (compaction pressure) illustrated a positive linear profile, factor D (water/cement ratio) affirmed a negative linear interaction profile. Compressive strength, therefore, depends on the interactive pattern between the two factors C and D.

### 2D process mapping plot

Contour/process plot, being a two-dimensional tool involved in the utilization of contour lines in the connection of points which resulted in the same response (Xu et al. 2016; Akinwande et al. 2022a, b). Contour plots show an interactivity outline between experimental variables and the response, exposing different regions or zones where varying response values can be attained at different experimental conditions.

Figure 5a demonstrates regions where varying compressive strengths are attained based on the interaction between GP percentage replacements and curing duration. An important region of concern in contour plots is the optimum region and, in this case, it is denoted as point A, where a strength range of > 6 MPa is realizable. The corresponding range of parameters is 21.49 to 49.50% for replacement proportion and 45.47 to 60 days curing age. Figure 5b indicates the contour plot of the interactivity existing between replacement proportion and compaction pressure as it affects the

response. The plot decodes varying values of the response feasible at the diverse combination of factors.

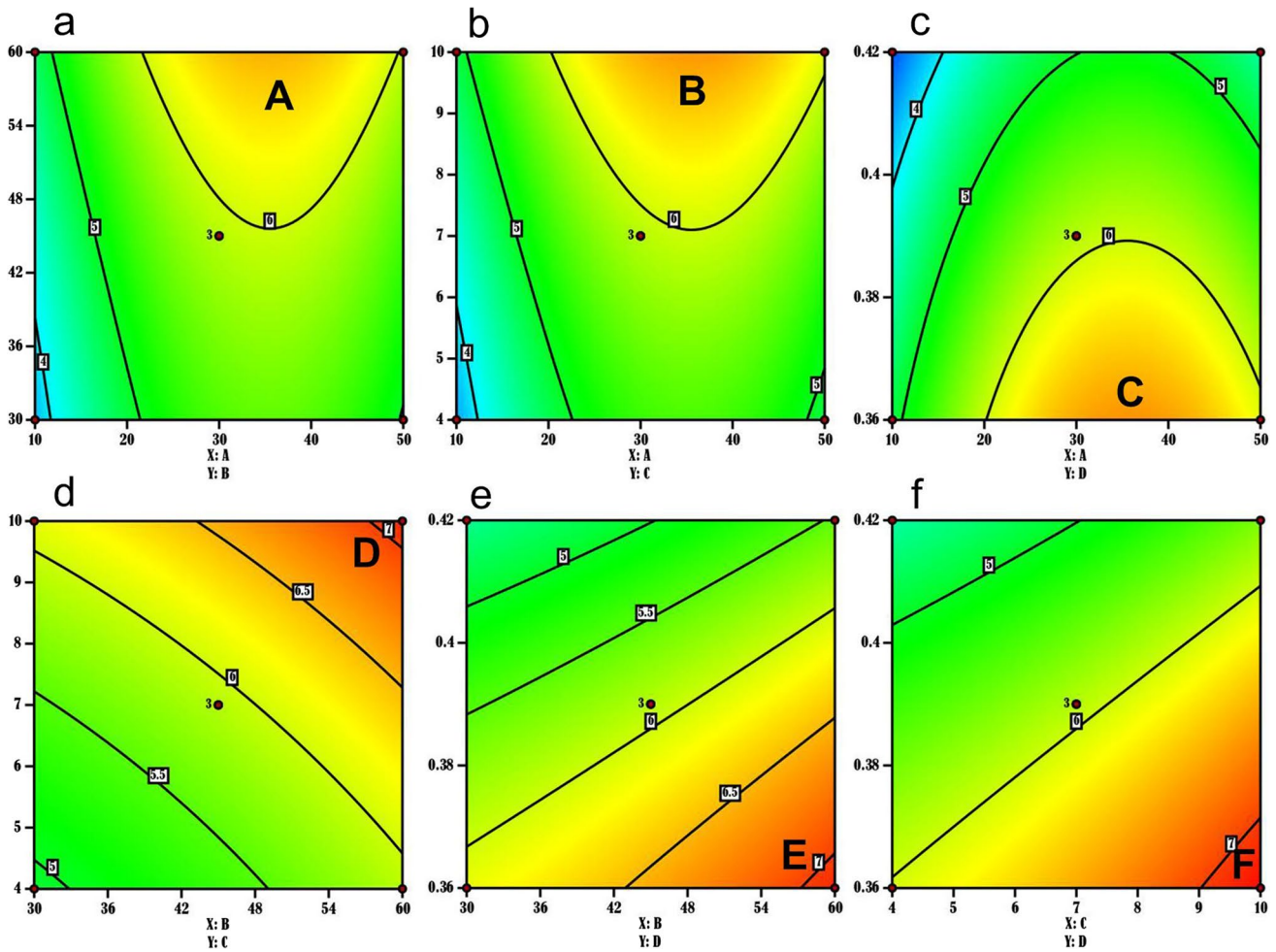
The optimum region (B) depicts a zone in which optimum response value > 6 MPa is viable at corresponding ranges of 20.22 to 50% for GP replacement proportion and 7.08 to 10 MPa compaction pressure.

Figure 5c features the contour plot of the combination of varying replacement proportions and water/cement ratio on compressive strength. The map revealed differing values of the compressive strength possible at the diverse combination of GP replacement proportion and water/cement ratio. Portion C is the optimum region where the optimum range for compressive strength > 6 MPa is feasible at corresponding factor inputs of 20.13 to 50% for GP replacement proportion and 0.36 to 0.39 for water/cement ratio. Figure 5d indicates the contour plot of the interaction curing duration vs compaction pressure with respect to compressive strength. The map depicts a diverse range of values for compressive strength reachable by the combination of curing duration and compaction pressure. Portion D being the optimum region, shows that compressive strength > 7 MPa is achievable with the corresponding factor combination of 57.41 to 60 days of curing and 9.57 to 10 MPa compaction pressure. Figure 5e presents zones in which diverse values of compressive strength are realized on account of the interaction between curing duration and water/cement ratio. The region marked E is the optimum zone where a strength value > 7 MPa can be achieved. The corresponding range of parameters is 57.27 to 60 days for curing duration and 0.36 to 0.366 water/cement ratio. Figure 5f indicates the contour plot of the interaction compaction pressure vs water/cement ratio as it affects the response. The plot depicts varying values of the reference feasible at the diverse combination of factors. The optimum region (F) shows the zone in which the optimum response value > 7 MPa is viable at corresponding ranges of 9.02 to 10 MPa for compaction pressure 0.36 to 0.37 water/cement ratio.

### Optimization and validation

The response surface method is a useful statistical tool for optimization of responses presenting the most desirable factor combination for a given response. Design-Expert 13 was employed in the optimization process with optimization criteria stipulated in Table 6. Factors A, B, C, and D were set in range while the goal was to maximize compressive strength with the lower/upper limit range. Optimum conditions for compressive strength optimization are presented in Fig. 6a which are 36.68% for GP replacement of cement, 57.82 days for curing duration, 8.50 MPa for compaction pressure, and 0.364 water/cement ratio. Optimum compressive strength of 7.358 MPa was predicted (Fig. 6b).





**Fig. 5** Contour map of the variation in responses at a varying range of process variables represented by **a** percentage replacement vs curing duration, **b** percentage replacement vs compaction pressure, **c** percentage replacement vs water/cement ratio, **d** curing duration vs

compaction pressure, **e** curing duration vs water/cement ratio, and **f** compaction pressure vs water/cement ratio. Here, A is percentage replacement (%), B is curing duration (days), C is compaction pressure (MPa), and D is water/cement ratio

**Table 6** Optimization criteria

Name	Goal	Lower limit	Upper limit	Lower weight	Upper weight
A: percentage replacement	Is in range	10	50	1	1
B: curing duration	Is in range	30	60	1	1
C: compaction pressure	Is in range	4	10	1	1
D: W/C ratio	Is in range	0.36	0.42	1	1
Compressive strength	Maximize	3.0	7.27	1	1

In the validation of the predicted optimum strength, five experimental runs were done employing the optimum conditions and a mean value was obtained. A mean value of 7.54 MPa was realized which is a deviation of 0.0247 or an error of 2.47% from the predicted value. The error is < 5% obtained value is regarded marginal and confirmed that there is a strong agreement between the predicted value and

experimental outcome, therefore, the model is validated and termed statistically fit.

The value of 7.54 MPa satisfied the minimum compressive strength value of 5.2 MPa as prescribed in BS 3921 (BS 3921 1985), 3.5 MPa minimum strength value for low rise-low cost building application stated in IS 2185 (IS 2185 2005). Equally met NIS 87 (NIS 87 2000) stipulated value of

Fig. 6 Optimization plot

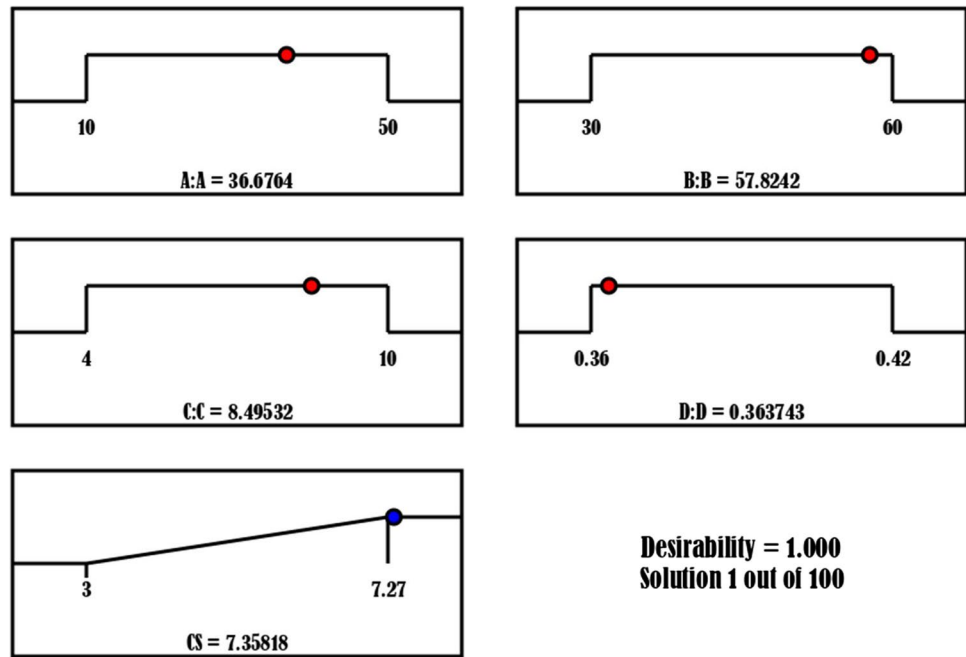


Table 7 Significance of glass powder input

Indicator	30	45	60
Reference mix	5.25	6.06	6.27
Optimum mix	5.94	7.09	7.54
% Difference between optimum mix and reference mix	13.1	33.0	24.0

2.85 MPa for minimum compressive strength and 4.14 MPa lowest strength value for non-load bearing wall bricks as per ASTM C 129–17 (ASTM C 129 2017) stipulation.

To evaluate the influence of glass powder as a cement supplement in paper-cement composite, the investigation was further carried on comparison between values of the reference mix cured for 30, 45, and 60 days and values of the optimized samples prepared at optimum conditions and cured for 30, 45, and 60 days. In order to access the influence of glass powder on the paperbricks, reference bricks was prepared with 40 wt.% cement and 20 wt.% sand. Optimum condition of compaction pressure of 8.50 MPa and water/cement ratio of 0.364 were employed in the preparation of the sample. Optimum mix was also produced at optimum condition cement content of  $(100-36.68) \times 40\%$  cement,  $25.33 \times 40\%$  GP, 20% sand. Optimum mix is therefore rewritten as 25.32% cement, 14.67% GP, 20% sand. Similar to the reference mix, the optimum mix was prepared at compaction pressure of 8.50 MPa and water/cement ratio of 0.364. The specimen were cured for 30, 45, and 60 days.

From Table 7, it is observed that reference mix prepared with 40% cement had compressive strengths of 5.25, 6.06,

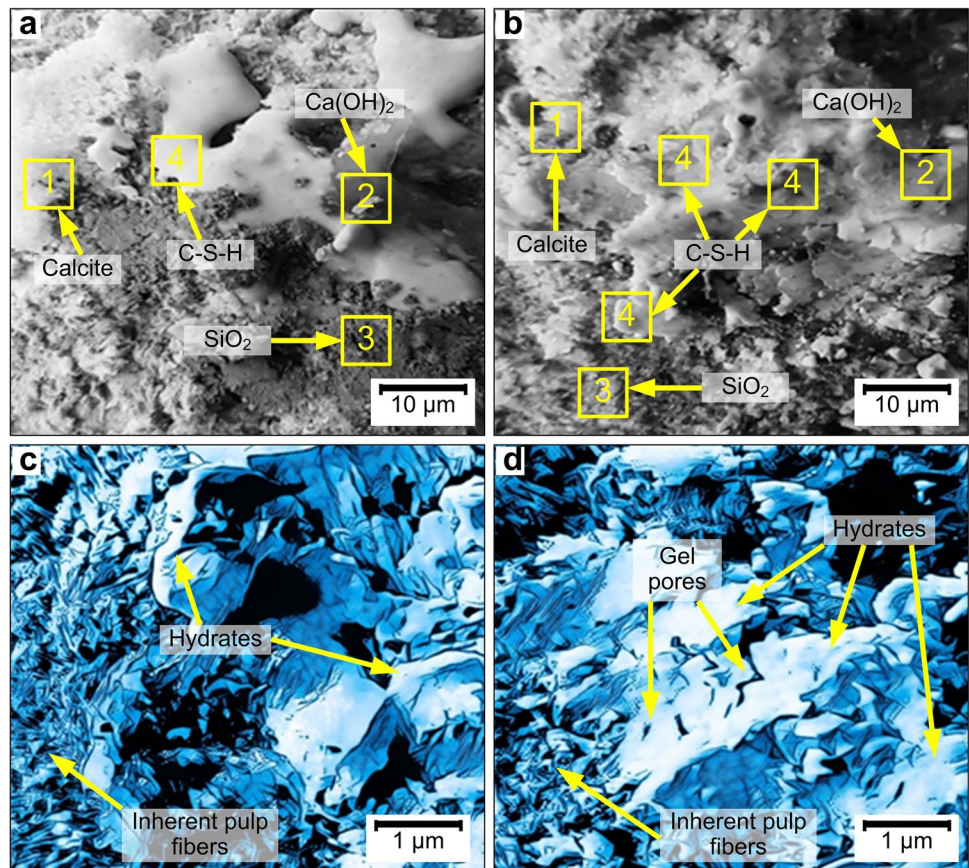
and 6.27 MPa at 40, 45, and 60 days. Under 30 days curing, there was 9.33% increase in strength as result of GP replacement of cement. Under 45 days, the difference was 19.96% increase in strength while 60 days curing yielded 16.59%. The outcome indicate GP as a good cement replacement which not only maintained the strength of the bricks but also enhanced the strength. The feat is linked to execution of pozzolainc reaction within the matrix during hydration which led to conversion of hydrated lime to calcium silicate hydrate. Optimum improvement was achieved at 45 days, which may mean optimum period for pozzolanic reaction for waste glass in paperbricks is 45 days; however, more study need to be carried out in this regards to confirm or disregard the postulation.

### Microstructural analysis

Figure 7 features the microstructural image of reference mix prepared with 40% cement, 20% sand, water/cement ratio 0.364 compacted at 8.50 MPa and cured for 60 days (no waste glass dosage) and optimized sample prepared at optimum conditions of 36.68% GP replacement of cement, curing duration of 60 days, compaction pressure of 8.50 MPa, and the water-cement ratio of 0.36. Figure 7a shows the SEM image of the reference paperbricks. Hydrate phases are observed which normally contribute to the strength of cement composite (Dunuweera and Rajapakse 2018). Majorly observed features are calcite, hydrated lime, quartz and calcium silicate hydrate. The features were affirmed by the spot EDX analysis carried out on labelled points 1, 2, 3, and 4 further compared with the result of X-ray



**Fig. 7** SEM and blue ray fluorescence microstructural image of **a** reference specimen prepared with 40 wt.% cement and **b** optimum sample prepared at optimum condition



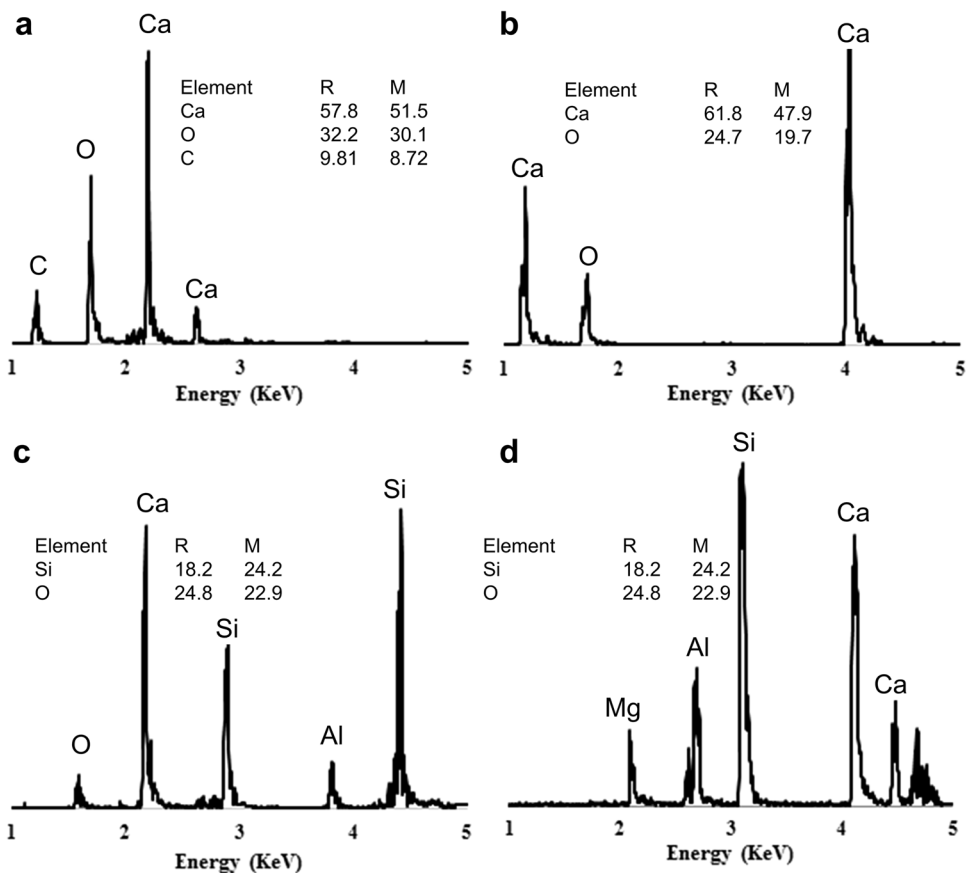
diffraction carried out on the samples. As initially explained, about 25% of hydration products are portlandite which has little contribution to strength when compared with calcium silicate hydrate (C-S-H). A higher proportion of hydrated lime is observed with Fig. 7a relative to Fig. 7b. In Fig. 7b (optimized sample), lesser portlandite is observed, owing to the pozzolanic reaction as a result of the presence of glass powder which converted more  $\text{Ca(OH)}_2$  to C-S-H. This outcome is reflected in the strength value of the optimized yielding 25.7% improvement over the reference mix.

Other features observed in the figures (Fig. 7a, b) are calcite and quartz.  $\text{CaCO}_3$  increases early strength in cement composites on account of high hydration rate, yet, at a more matured age, the contribution is reduced, taken over by calcium silicate hydrate. Therefore, more C-S-H phases at older ages are necessary. Comparing the images of the reference mix and optimized mix, a lower proportion of  $\text{CaCO}_3$  is observed in the optimized mix than the reference. This is as a result of hydration reaction producing more of C-S-H, thereby increasing C-S-H/Calcite ratio in the matrix consequence of which contributed to improved strength in the optimized sample with respect to the reference mix. More so, the pozzolanic reaction reduced the carbonation reaction (reaction of  $\text{CaO}$  with  $\text{CO}_2$ ) thereby reducing the volume of calcite formed in the optimized sample, reflecting in the

better strength performance at 60-day curing duration (Ali et al. 2015; Swaidani et al. 2017). Quartz is also another phase identified, which contributes to the strength of the samples. Figure 7a and b present the polarized (blue ray) fluorescence image of the two samples (reference and optimized sample) featuring hydration products, gel pores, and inherent pulp fiber distribution within the matrix.

Figure 8 presents the element composition of identified spots in both reference and optimized sample (Fig. 7), confirming the phases observed. Figure 8a shows the elemental component for spot 1. Major elements identified are calcium, carbon, and oxygen depicting the presence of calcite. Comparison between reference mix and optimized mix shows that Ca, C, and O are in higher proportion in the reference mix than optimized mix depicting the higher proportion of calcite in D than in M. Therefore, pozzolanic reaction, as a result of GP addition ensured lower calcite in M, contributing to higher 60-day strength in M compared to D. Figure 8b illustrates the presence of Ca and O identifying the presence of hydrated lime in spot 2. In comparison, the proportion of the elements are higher in the reference sample than the optimized sample showing a higher presence of lime in the reference mix. The feat is based on pozzolanic reaction converting lime to C-S-H. In Fig. 8c, peaks of silicon are pinpointed coupled with that of oxygen for spot 3, establishing the

**Fig. 8** Elemental analysis and comparison between reference and optimized mixed by spot energy-dispersive spectrometry identifying **a** CaCO<sub>3</sub>, **b** Ca(OH)<sub>2</sub>, **c** SiO<sub>2</sub>, and **d** C-S-H



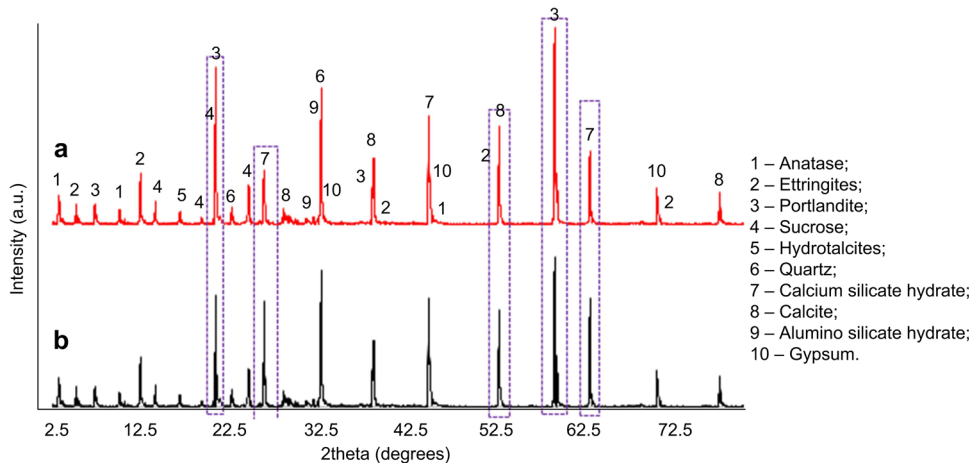
presence of quartz. Going by the proportion of the element in both samples, more silicon is identified in the optimized sample than reference sample. This observation is hinged on the presence of the glass powder (silica-based) contributing more silicon presence for reaction. Elemental features of spot 4 are clearly represented in Fig. 8d. Peaks of calcium, aluminum, and silicon exhibit the presence of calcium silicate and calcium aluminate hydrates and since higher peaks of silicon are portrayed, more of C-S-H is present. A higher

amount of calcium, aluminum, and silicon were present in the optimized sample relative reference sample; therefore, higher calcium silicate hydrate and alumino silicate hydrate are associated with the optimized sample.

**XRD analysis**

XRD phase identification of reference and the optimized sample is demonstrated in Fig. 9. Figure 9a present identified

**Fig. 9** XRD phase identification of composites representing **a** referent mix and **b** optimized mix



phase in the reference mix. High peaks of ettringites ( $12.6^\circ$ ,  $36.1^\circ$ ,  $50.3^\circ$ , and  $73.8^\circ$ ), portlandite ( $7.8^\circ$ ,  $19.4^\circ$ ,  $36.7^\circ$ , and  $58.6^\circ$ ), calcium silicate hydrate ( $27.8^\circ$ ,  $44.6^\circ$ ,  $62.5^\circ$ ), calcite ( $38.4^\circ$ ,  $52.6^\circ$  and  $82.4^\circ$ ), and quartz ( $20.2^\circ$ ,  $32.8^\circ$  and  $52.6^\circ$ ) are observed to be present at respective  $2\theta$  values highlighted in the brackets. These hydration products are identified as symbolic cement hydration phases. Other phases noted are sucrose, anatase and hydrotalcite linked to alkaline hydrolysis of inherent pulp cellulose. Ettringites presence occur based on interactions of sulphate and aluminate phases.

The same features are repeated in the matrix of the optimized sample. The difference in height of the peaks is identified in the portions in purple color. Peak labeled 3 corresponding to  $2\theta$  equals  $19.4^\circ$  for portlandite which was reduced in the optimized sample as a result of a pozzolanic reaction involving the conversion of lime to calcium silicate hydrate (C–S–H) and calcium aluminate hydrate. Peaks corresponding to  $2\theta$  equals to  $27.8^\circ$  are attributable to calcium silicate hydrate. As observed, higher peaks are noted in the optimized sample, compared with the reference mix; therefore, it is deduced that glass powder replacement of cement ensued a higher proportion of C–S–H in the optimized mix as a result of the enabled pozzolanic activity. Peaks corresponding to  $52.6^\circ$  for calcite have lower value in Fig. 9b than Fig. 9a associated with a lower proportion of calcite in the optimized mix than reference mix, confirming results depicted by elemental analysis of the spot EDX and SEM image.

Likewise, peaks corresponding to  $58.6^\circ$  identified portions of portlandite which has a lower peak in Fig. 9b relative to Fig. 9a. This confirms that lower portlandite is present in the optimized sample relative to the reference sample corroborating results presented in SEM images and elemental analysis. The peak corresponding to  $62.6^\circ$  depicts peaks of calcium silicate hydrate. A higher peak is pictured in Fig. 9b as compared with Fig. 9a confirming a higher C–S–H portion in the optimized sample relative to a reference sample. The result corroborated the SEM and elemental analysis earlier discussed.

## Conclusions

This study involved the development of paperbricks by optimization of the processing parameters; GP replacement of cement (A), curing duration (B), compaction pressure (C), and water/cement ratio (D). Response surface method (RSM) was employed and experimental design was undergone by Box Behnken approach. Following conclusions are arrived at.

- Results of the ANOVA showed that factors A, B, C, and D had a significant effect on compressive strength response.
- The order of significance of the parameters are water/cement ratio, cement replacement, compaction pressure,

and curing duration with values of 27.21, 15.74, 15.56, and 10.61% contributions, respectively.

- Water/cement ratio had an antagonistic effect on the response while curing duration, cement replacement, and compaction pressure showed a synergetic effect on the response.
- The quadratic model for the prediction of compressive strength as a function of the parameters was developed and validated.
- Response surface plots for the interactions affirmed the response is dependent on the interactive pattern of the factors. The contour plots also depict varying ranges of response values attainable at different combinations of factors.
- Optimal compressive strength response for the paperbricks was attained at operating conditions of 36.68%, 57.82 days, 8.50 MPa, and 0.364 for factors A, B, C, and D in that order. The predicted optimal compressive strength was 7.358 MPa.
- Validation experiment carried out at the optimum conditions yielded 7.54 MPa, a deviation of  $-0.0247$  and since the deviation is less than  $\pm 0.05$ , the model was accepted as statistically fit for prediction of response at varying conditions. The validated value satisfied the various requirement for low-cost building.

Conclusively, paperbricks can be developed by the blend of waste paper and glass powder at stipulated optimal conditions.

**Acknowledgements** Authors appreciate the Department of Metallurgical and Materials Engineering and Department of Industrial Design, Federal University of Technology, Akure, Ondo State, Nigeria; Department of Construction and Wood Technology, Akenten Appiah-Menka University of Skills Training and Entrepreneurial Development, Kumasi, Ghana; Ministry of Science and Higher Education of the Russian Federation in the framework of Increase Competitiveness Program of NUST «MISiS», implemented by a governmental decree dated March 16, 2013, N 211.

**Author contribution** A.A. Akinwande: conceptualization, methodology, investigation, formal analysis, data curation, writing—original draft, writing—review and editing. D.O. Folorunso: methodology, investigation, formal analysis, data curation, writing—original draft, writing—review and editing. O.A. Balogun: data curation, methodology, investigation, formal analysis, writing—review and editing. H. Danso: data curation, methodology, investigation, formal analysis, writing—review and editing. V. Romanovski: data curation, methodology, investigation, visualization, formal analysis, writing—review and editing.

## Declarations

**Ethics approval and consent to participate** Not applicable.

**Consent for publication** Not applicable.

**Conflict of interest** The authors declare no competing interests.

**Data availability** All data employed in support to the outcomes in the study are included in this article.



## References

- Ahmad A, Adil M, Khalil A, Rahman M (2021) Mechanical properties and durability of boadcrete blocks prepared from recycled cardboard. *J Build Eng* 33:101644. <https://doi.org/10.1016/j.jobe.2020.101644>
- Akinwande AA, Adediran AA, Balogun OA, Olusoji OS, Adesina OS (2021a) Influence of alkaline modification on selected properties of banana fiber paperbricks. *Sci Rep* 11(5793):1–19. <https://doi.org/10.1038/s41598-021-85106-8>
- Akinwande AA, Adediran AA, Balogun OA, Adesina OS, Olasoji OS, Owa AF, Erinle TJ, Akinlabi ET (2021b) Assessment of alkaline treatment of palm kernel fiber and curing duration on selected properties of cement-paper composite boards. *Cogent Eng* 8(1909690):1–25. <https://doi.org/10.1080/23311916.2021.1909690>
- Akinwande AA, Balogun OA, Valentin R (2022a) Modeling, multi-response optimization, and performance reliability of green metal composites produced from municipal wastes. *Environ Sci Pollut Res*. <https://doi.org/10.1007/s11356-022-20023-5>
- Akinwande AA, Folorunso DO, Balogun OA, Valentin R (2022b) Mathematical modelling, multi-objective optimization, and compliance reliability of paper-derived ecocomposites. *Environ Sci Pollut Res*. <https://doi.org/10.1007/s11356-022-20714-z>
- Ali M, Abdullah MS, Saad SA (2015) Effect of calcium carbonate replacement on workability and mechanical strength of Portland cement concrete. *Adv Mater Res* 1155:137–141. <https://doi.org/10.4028/www.scientific.net/AMR.1115.137>
- Arya RK, Kansal R (2015) Utilization of waste papers to produce eco-friendly bricks. *Int J Sci Res* 5(8):92–96
- ASTM C 129 (2017) Standard specification for nonloadbearing concrete masonry units. ASTM International, West Conshohocken
- ASTM C 192/C 192M (2019) Standard practice for making and curing concrete test specimens in the laboratory. ASTM International, West Conshohocken
- ASTM C 618 (2019) Standard specification for coal fly ash and raw or calcined natural pozzolan for use in concrete. ASTM International, West Conshohocken
- Babu CCS, Kumar LP, Reddy KDK, Farooq AM, Vandrakanth V (2019) An experimental study on papercrete bricks. *J Emerg Technol Innov Res* 6(4):167–177
- Bakhsh EM, Khan ShB, Akhtar K, Danish EY, Fagieh TM, Qiu Ch, Sun Y, Romanovski V, Su X (2022) Simultaneous preparation of humic acid and mesoporous silica from municipal sludge and their adsorption properties for U(VI). *Colloids Surf A* 647:129060. <https://doi.org/10.1016/j.colsurfa.2022.129060>
- BS 3921 (1985) British standard specification for clay bricks. British Standard Group, UK
- Carbo EG, Soriano L, Flores MR, Serna P (2021) Characteristics of glass powder from glass recycling process waste and preliminary testing. *Materials* 14(2971):1–15. <https://doi.org/10.3390/ma14112971>
- Danso H (2015) Influence of compaction rate on the strength properties of compressed earth blocks. *Adv Mater Sci Eng* 2016(8780368):1–8. <https://doi.org/10.1155/2016/8780368>
- Delcasse MM, Rahul V, Abhilash C, Pavan MK (2017) Papercrete bricks an alternative sustainable building material. *Int J Eng Res App* 7(3):9–14
- Devi RR, Umlong IM, Das B, Borah K, Thakur AJ, Raul PK, Banerjee S, Singh L (2013) Removal of iron and arsenic (III) from drinking water using oxide-coated sand and limestone. *Appl Water Sci*. <https://doi.org/10.1007/s13201-013-0139-5>
- Dunuweera SP, Rajapakse RMG (2018) Cement types, composition, uses and advantages of nano cement, environmental impact on cement production and possible solutions. *Smart Build Constr Mater* 4158682:1–11. <https://doi.org/10.1155/2018/4158682>
- Ebadi SV, Fakhrali A, Semnani D (2019) Systematic investigation of parameters of an electrospinning process of poly(acrylic acid) nanofibers using response surface methodology. *Bull Mater Sci* 42(115):1–10. <https://doi.org/10.1007/s12034-019-1764-x>
- Ferronato N, Torretta V (2019) Waste mismanagement in developing countries: a review of global issues. *Int J Environ Res Public Health* 16(1060):1–28. <https://doi.org/10.3390/ijerph16061060>
- Hurynovich A, Kwietniewski M, Romanovski V (2021) Evaluation of the possibility of utilization of sewage sludge from Wastewater Treatment Plant – case study. *Desalin Water Treat* 227:16–25. <https://doi.org/10.5004/dwt.2021.27199>
- Husuma HS, Mahfud M (2016) Response surface methodology for optimization studies of microwave-assisted extraction of sandalwood oil. *J Mater Environ Sci* 7(6):1958–1971
- IS 2185 (2005) Concrete masonry units, part 1; hollow and solid concrete blocks. Bureau Indian Stand, New Delhi
- IS 383 (1970) Specification for coarse and fine aggregates from natural sources for concrete. Bureau of Indian Standards, New Delhi
- IS 516 (2004) Method of tests for strength of concrete. Bureau of Indian Standards, New Delhi
- IS 8112 (2013) Specification for 43 grade ordinary portland cement. Indian Bureau of Standard, New Delhi
- Jeyakumar MSB, Raju VK (2019) Characteristics of paperbricks and inequitable substitution of cement. *Int J Innov Technol Expl Eng* 8(125):85–88. <https://doi.org/10.35940/ijitee.1.1026.10812S19>
- Joshua PB, Glanda GG (2016) Slum conditions in urban Nigeria: a case of Jimeta-Yola, Adamawa State, Nigeria. *J Environ Earth Sci* 6(3):74–80
- Kamarou M, Korob N, Romanovski V (2021a) Structurally controlled synthesis of synthetic gypsum derived from industrial wastes: sustainable approach. *J Chem Technol Biotechnol* 96(11):3134–3141. <https://doi.org/10.1002/jctb.6865>
- Kamarou M, Korob N, Hil A, Moskovskikh D, Romanovski V (2021b) Low-energy technology for producing anhydrite in the  $\text{CaCO}_3 - \text{H}_2\text{SO}_4 - \text{H}_2\text{O}$  system derived from industrial wastes. *J Chem Technol Biotechnol* 96(7):2065–2071. <https://doi.org/10.1002/jctb.6740>
- Kassa Y (2019) Application of cane molasses as concrete retarder admixture. *SN Appl Sci* 1(1547). <https://doi.org/10.1007/s42452-019-1608-8>
- Khare M, Gupta RK, Bhardwaj B (2018) Development of empirical relationship for surface roughness during machining of metal matrix composite. *IOP Conf Ser: Mater Sci Eng* 402:012010
- Liladia Y, Malviga S, Baig A (2020) Utilization of paper to produce bricks. *Int Res J Eng Technol* 7(2):1259–1263
- Mandilli B, Taqi M, Chakir H, Douzane O, Errouaiti M (2020) Development of new construction material for thermal insulation of building based on aggregate of waste paper and cement. *Heat Mass Transf*. <https://doi.org/10.1007/s00231-020-02811-2>
- Matsukevich I, Kulinich N, Romanovski V (2022) Direct reduced iron and zinc recovery from electric arc furnace dust. *J Chem Technol Biotechnol*. <https://doi.org/10.1002/jctb.7205>
- Mohammed M, Shafiq N, Abdallah NAW, Ayoub M, Haruna A (2020) A review on achieving sustainable construction waste management through application of 3R (reduction, reuse and recycling). A lifecycle approach. *IOP Conf Ser: Earth Environ Sci* 476:1–10. <https://doi.org/10.1088/17551315/476/1/012010>
- Muttashar HL, Ali NB, Ariffin MAM, Hussin MW (2018) Microstructural and physical properties of waste garnets a promising construction material. *Case Stud Constr Mater* 8:87–96. <https://doi.org/10.1016/j.cscm.2017.12.001>
- Najad AJA, Kareem JKH, Azline N, Ostovar N (2019) Waste glass as partial replacement in cement – A review. *IOP Conf Ser: Earth*

- Environ Sci 357:012023. <https://doi.org/10.1088/1755-1315/357/1/012023>
- NIS 87 (2000) NIS. 87, Standards for sandcrete blocks. Nigerian Industrial Standards
- Nyantakyi EK, Obiri-Yeboah A, Mohammed GA, Domfeh MK, Obeng-Ahenkora NK (2020) Partial replacement of cement with glass bottle waste powder in concrete for sustainable waste management: a case study of Kumasi metropolitan assembly, Ashanti region, Ghana. *J Civ Eng Res* 10(2):29–38. <https://doi.org/10.5923/j.jce.20201002.01>
- Obaitor OS, Lawanson TO, Stellmes M, Lakes T (2021) Social capital: higher resilience in slums in the Lagos metropolis. *Sustainability* 13(3879):1–18. <https://doi.org/10.3390/su13073879>
- Ofori P (2020) Housing poverty in developing countries: challenges and implications for decent accommodation in Swedru, Ghana. *Acta Structilia* 27(2):57–92. <https://doi.org/10.18820/24150487/as27i2.3>
- Okeyinka OM, Oloke DA, Jamal K (2015) Development of environmentally friendly lightweight block from waste paper. 2<sup>nd</sup> International Sustainable Building Symposium, Gazi University. 28–30 May, 2015. Ankara Turkey
- Olofinnade OM, Ede AN, Ndambuki JM, Ngene BU, Akinwunmi II, Ofuyatan O (2018) Strength and microstructural of eco-concrete produced using waste glass as partial and complete replacement for sand. *Cogent Eng* 5(1):1483860. <https://doi.org/10.1080/23311916.2018.1483860>
- Panda S, Sarkar P, Davis R (2020) Effect of water-cement ratio on mix design and mechanical strength of copper slag aggregate concrete. *IOP Conf Ser: Mater Sci Eng* 936:012019. <https://doi.org/10.1088/1757-8899X/936/1/012019>
- Pona HT, Xiaoli D, Ayantobo OO, Tetteh ND (2021) Environmental health situation in Nigeria: current status and future needs. *Heliyon* 7:e06330. <https://doi.org/10.1016/j.heliyon.2021.e06330>
- Rani V, Vikram E, Kumar ES (2018) Development of ecofriendly lightweight brick using waste paper. *Int J Technol Res Eng* 5(10):4074–4078
- Raoelivololona T, Ramarason M, Raninosa C (2020) Paper recycling for the making of construction materials. *MATEC Web Conf* 307(01041):1–5. <https://doi.org/10.1051/mateconf/202030701041>
- Romanovski V, Romanovskaia E, Moskovskikh D, Kuskov K, Likhavitski V, Mehmet FA, Beloshapkin S, Matsukevich I, Khort A (2021a) Recycling of iron-rich sediment for surface modification of filters for underground water deironing. *J Environ Chem Eng* 9(4):105712. <https://doi.org/10.1016/j.jece.2021.105712>
- Romanovski V, Klyndyuk A, Kamarou M (2021b) Green approach for low-energy direct synthesis of anhydrite from industrial wastes of lime mud and spent sulfuric acid. *J Environ Chem Eng* 9(6):106711. <https://doi.org/10.1016/j.jece.2021.106711>
- Romanovski V, Zhang L, Su X, Smorokov A, Kamarou M (2022) Gypsum and high quality binders derived from water treatment sediments and spent sulfuric acid: chemical engineering and environmental aspects. *Chem Eng Res Des* 184:224–232. <https://doi.org/10.1016/j.cherd.2022.06.008>
- Sadiqul Islam GM, Rahman MH, Kazi N (2017) Waste glass powder as partial replacement of cement for sustainable concrete practice. *Int J Sustain Built Environ* 6:37–44. <https://doi.org/10.1016/j.ijbsbe.2016.10.005>
- Sangrutsamee V, Srichandr P, Poolthong N (2012) Re-pulped waste paper-based composite building materials with low thermal conductivity. *J Asian Architect Build Eng* 11(1):147–157. <https://doi.org/10.3130/jaabe.11.147>
- Shabani N, Hamadian M, Ghasemi AR, Sarafrazi M (2018) Physicochemical and mechanical properties of epoxy/polyurethane/nickel manganite nanocomposite: a response surface methodology/central composite design study. *J Inorg Organomet Polym Mater*. <https://doi.org/10.1007/s10904-018-0931-7>
- Shahidkha PB, Singh VV (2018) Using molasses in concrete as a time retarding admixture. *Int J Adv Res* 6(6):1053–1060. <https://doi.org/10.21474/IJAR01/7310>
- Silantsev AA, Vildanov AI, Kuzmin EV (2019) Statistical simulation of signal to noise ratio estimation. *J Fundam Appl Sci* 10(2S):571–578. <https://doi.org/10.4314/jfas.v10i2s.41>
- Solaja OM, Awobona S, Omodehin AO (2020) Knowledge and practice of recycled plastic bottles (RPB) built homes for sustainable community-based housing projects in Nigeria. *Cogent Soc Sci* 6(1778914):1–20. <https://doi.org/10.1080/23311886.2020.1778914>
- Swaidani AA, Soud A, Hammami A (2017) Improvement of the early-age compressive strength, water permeability and sulphuric acid resistance of scoria-based mortars/concrete using limestone filler. *Adv Mater Sci Eng* 8373518:1–17. <https://doi.org/10.1155/2017/8373518>
- Tamanna N, Sutan NM, Tuladhar R, Ching Lee DT, Yakub I (2016) Pozzolanic properties of glass powder in cement paste. *J Civ Eng Sci Technol* 7(2):75–81
- Wang XY (2019) Analysis of hydration and optimal strength combinations of cement-limestone-metakaolin ternary composite. *Adv Mater Sci Eng* 8361810:1–13. <https://doi.org/10.1155/2019/8361810>
- Wang M, Zhang B, Li G, Wu T, Sun D (2019) Efficient remediation of crude oil-contaminated soil using solvent/surfactant system. *RSC Adv* 9:2402–2411. <https://doi.org/10.1039/c8ra09964b>
- World Bank (2018) Project information/Document/Integrated Safeguards data sheet (PID/ISDS), Nigeria. Affordable Housing Project (P 165296), 1–14
- Xu B, Chen J, Yao M (2016) Identification of contour lines from average quality scanned topographic maps. *Math Probl Eng* 3089690:1–14. <https://doi.org/10.1155/2016/3089690>
- Zaki HM (2019) Characteristics of paper-cement composite. *J Eng* 25(4):122–138. <https://doi.org/10.31026/j.eng.2019.04.09>
- Zalyhina V, Cheprasova V, Romanovski V (2021a) Pigments from spent chloride-ammonium zinc plating electrolytes. *J Chem Technol Biotechnol* 96(10):2767–2774. <https://doi.org/10.1002/jctb.6822>
- Zalyhina V, Cheprasova V, Belyaeva V, Romanovski V (2021b) Pigments from spent Zn, Ni, Cu, and Cd electrolytes from electroplating industry. *Environ Sci Pollut Res* 28:32660–32668. <https://doi.org/10.1007/s11356-021-13007-4>
- Zalyhina V, Cheprasova V, Romanovski V (2022) Paper industry slag for the production of building ceramics. *J Chem Technol Biotechnol*. <https://doi.org/10.1002/JCTB.7174>
- Zhang L, Yue Y (2018) Influence of waste glass powder usage on the properties of alkali-activated slag mortars based on response surface methodology. *Constr Build Mater* 181:527–534. <https://doi.org/10.1016/j.conbuildmat.2018.06.040>
- Zhang L, Zhai J (2020) Application of response surface methodology to optimize alkali-activated slag mortar with limestone powder and glass powder. *Struct Concr* 1–12. <https://doi.org/10.1002/suco.202000018>
- Zheng K (2016) Pozzolanic reaction of glass powder and its role in controlling alkali-silica reaction. *Cement Concr Compos* 67:30–38. <https://doi.org/10.1016/j.cemconcomp.2015.12.008>

**Publisher's note** Springer Nature remains neutral with regard to jurisdictional claims in published maps and institutional affiliations.

Springer Nature or its licensor holds exclusive rights to this article under a publishing agreement with the author(s) or other rightsholder(s); author self-archiving of the accepted manuscript version of this article is solely governed by the terms of such publishing agreement and applicable law.